

# Modelling the dynamics of soil macroporosity

## Abstract

Many factors affect soil porosity but major of them are soil fauna, plant roots and the climate. Many studies attempted to investigate the effect of these factors on the evolution of soil porosity separately. The objective of ~~is~~ this study is, based on an in situ experiment including three major porosity factors, propose a model of soil macroporosity evolution. In situ observation and quantification of the evolution of macroporosity under the influence of each agent separately and the three agents combined allow to propose a model for each case. Mathematical algorithms and computing are necessary to formalise this model and longterm experiment is needed to validate this model.

*Keywords:* Differential equations, Soil structure, Earthworms, Casts production, Swelling Shrinkage, Plant roots

---

## 1. Introduction

2 Soil, due to its importance in furnishing ecosystem services, attracted the  
3 attention of many soil scientists for many years. Many processes occurring in  
4 soil are defined and characterized but to better understand the fate of impor-  
5 tant factors, modelling approach has been developed. Since then, a various  
6 models concerning soil processes were developed and a historical point of  
7 view of this modelling is given by Vereecken et al. (2016). Among these  
8 processes soil structure, defined as the rearrangement of solid soil particles  
9 got a great interest. The consequence of this arrangement is the formation

10 of aggregates and voids. Many studies highlight the main factors that  
11 influence soil structure and the five major of them are i) soil fauna, ii) plant  
12 roots, iii) environmental factors, iv) inorganic binding agents and v) soil mi-  
13 croorganisms (Six et al., 2004). Research have been led to investigate  
14 the role of different agents on the evolution of structure. Plant roots influ-  
15 ence soil structure in different ways but the most studied is by introducing  
16 organic matter. This process is widely investigated and some models have  
17 been proposed. For example, Roth-C study the soil organic matter turnover  
18 in non-waterlogged soils (Coleman and Jinkinson, 1999) and how this pro-  
19 cess is involved in soil structure (aggregation formation). Based on Roth-C,  
20 Malamoud et al. (2009) proposed a new model which studies the dynamics  
21 of soil structure (aggregation and porosity) named Structure-C. This model  
22 written in Matlab consists of three sub models. An aggregation submodel,  
23 organic matter submodel and porosity submodel. The porosity submodel  
24 predicts the evolution of porosity during time under specific conditions of  
25 soil organic matter turnover.

26 Apart from its action in creating structure by introducing organic matter  
27 in soil, plant roots also enmesh soil particles and creates aggregates between  
28 what pores are created. This aspect of research is not widely explored. Nev-  
29 ertheless, the process is detailed by Jangorzo et al. (2015). A more complex  
30 modelling platform has been developed to help understanding and simulate  
31 major processes governing soil evolution. This platform named Virtual Soil  
32 or Vsoil (Lafolie et al., 2015) is designed to facilitate modelling chemical,  
33 physical and biological interactions occurring in soils and improve the simu-  
34 lation of anthropic activities and climate change impact on the soil ecosystem  
35 services. Different contributors may work together in order to develop mod-  
36 ules that can be incorporated in the platform. Since then, module of organic  
37 matter turnover, water dynamics are developed. An important module to de-  
38 velop will be that which concern the dynamic of soil structure (porosity and  
39 aggregation). Such a module exists, example Structure-C developed based  
40 on Roth-C. It describes the evolution of soil structure under the influence  
41 of soil organic matter dynamics and the agents that condition this evolution  
42 (Malamoud et al., 2009). This model does not take into account the fact  
43 that soil porosity evolves according to the influence of other major processes  
44 like earthworm activities as well as the physical process occurring in soil like  
45 swelling and shrinkage. The role of earthworms in soil structure is also widely  
46 studied and an attempt to model this process has been undertaken.

47 Another phenomenon that influence soil porosity is the wetting-drying

User  
2024-01-12 14:57:36

48 cycle related to property of swelling and cracking of the soil. Many stud-  
49 ies have been undertaken to study the process of soil cracking (Konrad and  
50 Ayad, 1997; Greco, 2002; Braudeau and Mohtar, 2006; Peng and Horn, 2007;  
51 Chertkov, 2012b,a) and its impact on soil porosity (Coppola et al., 2012,  
52 2015). In a recent work, Stewart et al. (2016) showed that most of mod-  
53 els developed do not consider the process in its whole. However, the total  
54 porosity produced during soil cracking in a swelling soil could be apportioned  
55 in three parts: aggregates porosity, shrinkage cracks and vertical subsidence  
56 and then proposed a unified model. There is an ongoing debate concerning  
57 the vertical subsidence as part of soil porosity in a swelling soil. However, we  
58 assume that the vertical subsidence is taken into account when considering  
59 the decrease of aggregates porosity during soil compaction. Moreover, the  
60 model of Stewart did not consider the repeating wetting-drying process or a  
61 successive swelling-shrinkage which naturally happened in a Vertisol. This  
62 why he assumed that the mass movement and erosion were insignificant.  
63 But, in a wetting-drying cycle, mass movement is the major driver of cracks  
64 dynamic (Jangorzo et al., 2015). Nevertheless, a part of this model could be  
65 integrated in a new model development by considering it as the state of the  
66 porosity in the first swelling-shrinkage process.

67 Two mechanisms drive the swelling-shrinkage cycle in soil. Mechanical  
68 loading mechanism and the second associated with the change in suction  
69 known as hydraulic loading mechanism (Wang and Wei, 2014). Mecha-  
70 nism of reversible swelling-shrinkage strain and the Mechanism of irreversible  
71 swelling-shrinkage strain (Wang and Wei, 2014) shows the behaviour of soil  
72 volume during swelling-shrinkage cycle. This volume is assumed to be irre-  
73 versible (Tessier, 1984; Jangorzo et al., 2015) in natural conditions. More the  
74 drying is important less the soil uptake water during wetting which means  
75 that the soil will swell less (volume decrease) (Croney and Coleman, 1954).  
76 Earthworm, considered as ecosystem engineer (Jones et al., 1994) have been  
77 widely studied in the context of their role in soil structure. The efficiency  
78 of these engineers (activity), particularly earthworms depends on three fac-  
79 tors (Kretzschmar, 1991). However, earthworms are more active in a range  
80 of water potential, when soil is loose and depending on the period of year.  
81 This activity conditioned the effect of this engineer on soil structure as the  
82 latter depends on the intensity of burrowing (Jangorzo et al., 2015). Ac-  
83 tivity of earthworm is also conditioned by soil temperature and individual  
84 mass of the organism (Kaneda et al., 2016). Based on laboratory and field  
85 experiments, many models have been developed to predict the role of some

86 earthworm species in soil aggregation (e.g. Kaneda et al., 2016) or in soil  
 87 carbon sequestration (e.g. Komarov et al., 2017). But these models neither  
 88 they did not predict the evolution of soil porosity nor they did not consider  
 89 the synergy that exist between plant roots and earthworm in soil structure  
 90 (Zangerlé et al., 2011; Jangorzo et al., 2015). One of the factor that most  
 91 incites earthworm burrowing is the food seeking. However, earthworm moves  
 92 into different layer of soil to find fresh organic matter that they decompose  
 93 and translocate sometimes deeper in the soil (Jangorzo, 2013). We could  
 94 then assume that more food is available, greater is the burrowing activity.  
 95 This assumption is modelled by Daniel (1991) when he studied the effect of  
 96 food consumption on aggregates formation. The degree of soil organic mat-  
 97 ter transformation by earthworm is conceptualized and modelled by Chertov  
 98 et al. (2017) and Komarov et al. (2017). If the soil aggregate formation is  
 99 known, it is not the case for the porosity existing in and between aggre-  
 100 gates. The aim of this work is to develop a mathematical integrated model  
 101 describing the porosity dynamics in model soils “constructed Technosols”.  
 102 This multi-agents model takes into account the effect of three ranked factors  
 103 -wetting-drying cycle, plant roots and soil fauna- (Jangorzo et al; 2017, data  
 104 not published) in the evolution of soil structure.

105 **2. Model theory**

106 *2.1. General model of soil porosity dynamics*

107 We hypothesis that the changes of macroporosity  $P$  with time  $t$ ,  $\frac{dP}{dt}$ ,  
 108 depends on the variation of macroporosity due to i) soil moisture, ii) the population dynamics of roots  $f(r)$ , and iii) the earthworm  
 109 respectively, as well as a porosity disappearance term  $D_P$ :

$$\frac{dP}{dt} = f(\Theta) + f(r) + f(w) - D_P. \tag{1}$$

111 *2.2. Changes in porosity due to variations in soil humidity (wetting and dry-*  
 112 *ing cycles)*

113 In clayey soils like Vertisols or in Technosols made of swelling materials  
 114 like paper or iron industry sludges, there are changes in soil porosity with  
 115 the variations of soil humidity (Peng and Horn, 2007; Huot et al., 2014,  
 116 BIOTECHNOSOL, others?). This shrinkage and swelling behaviour

User  
2024-01-12 15:22:39

---

User  
2024-01-12 15:24:13

117 When a soil is set up and watered, the first process that affects its porosity  
 118 is water loss. The behaviour of water movement in soil has been largely stud-  
 119 ied, particularly the process of swelling-shrinkage (Smiles, 2000). According  
 120 to its texture, soil swells when it is wetted which causes an increase of vol-  
 121 ume, a decrease of bulk density, and an increase in macroporosity (Smiles,  
 122 2000). Conversely, when the soil dries, it shrinks and its volume decreases  
 123 which leads to an increase of soil bulk density (Peng and Horn, 2007), a de-  
 124 crease of aggregates porosity (microporosity), and an increase of shrinkage  
 125 cracks (macroporosity) (Stewart et al., 2016). But, as the volume of cracks  
 126 is important, we assume that the total porosity of the soil increases as soon  
 127 as the water potential increases.

128 Stewart et al. (2016) have proposed and validated a unified model to  
 129 represent the variations of the different types of porosity with the  
 130 soil humidity. They consider three types of porosity:

131 In absence of any other agents, here we assume that the effect of  
 132 organisms is negligible, the main process that govern porosity formation is  
 133 water flow expressed by the swelling-shrinkage phenomenon. We used the  
 134 equation of Stewart et al. (2016) to model the variation of porosity due to  
 135 one wetting-drying cycle for cracks porosity:

$$\phi_{\text{crack}} = (\phi_{\text{pedon}} - \phi_{\text{min}}) \frac{1 - U^q}{1 - \epsilon U^q}, \quad (2)$$

136 with  $U = \Theta/\Theta_{\text{max}}$  and other parameters in Stewart et al. (2016).

137 Linking Stewart et al. (2016) equation with our framework:

$$f(\Theta) = \frac{\partial \phi_{\text{crack}}}{\partial t}. \quad (3)$$

138 We thus need to derivate  $\phi_{\text{crack}}$  with time  $t$ :

$$f(\Theta) = \frac{[-qU(t)^{q-1}U'(t)(1 + \epsilon U(t)^q)] - [q\epsilon U(t)^{q-1}U'(t)(1 - U(t)^q)]}{(1 - \epsilon U(t)^q)^2} \quad (4)$$

139 and  $U'(t) = \partial\Theta/\partial t$

$$f(\Theta) = (1 - \epsilon) \frac{[-qU(t)^{q-1}] - [2q\epsilon U(t)^{2q-1}]}{(1 - \epsilon U(t)^q)^2} \frac{\partial\Theta}{\partial t}, \quad (5)$$

140 where  $\epsilon$  and  $q$  are fitting parameters.

141 *2.3. Changes in porosity due to the dynamics of roots population*

142 Roots have three different impacts on porosity:

- 143 • firstly, they fill some available porosity while they are appearing and  
144 growing and then free up some pores when ageing and dying (by nar-  
145 rowing) and disappearing (by degrading); this affects macroporosity;
- 146 • secondly, when they are growing, they compact the neighbouring soil  
147 (rhizosphere) leading to a decrease of what Malamoud et al. (2009)  
148 called aggregates porosity or the soil microporosity. The intensity of  
149 compaction depends on either cracks exist before the appearance of  
150 roots or not; however, Jangorzo et al. (2015) showed that roots prefer-  
151 entially used existing pores like cracks when growing.
- 152 • third, when roots are degraded, they enter into the soil organic matter  
153 turnover which also has another impact of soil porosity as demonstrated  
154 by many authors (e.g. Coleman and Jinkinson, 1999; Malamoud et al.,  
155 2009).

156 In this model we only consider the effect of roots on the dynamics of macro-  
157 porosity by infilling.

158 Jangorzo (2013) and Jangorzo et al. (2015) have shown that the impact  
159 of roots on macroporosity depends on the age category of the roots. When  
160 young roots appear and then mature, they are growing thus leading to a  
161 decrease in porosity. During ageing and degradation after death, they are  
162 freeing some space which, by consequence lead to an increase in porosity.  
163 Thus when roots age and become old roots the porosity increases. Thus, if  
164 we consider the total surface fill by roots we can distinguish three different  
165 age categories:

- 166 • surface with young root  $R_y(t)$ ,
- 167 • surface with mature root  $R_m(t)$ ,
- 168 • surface with old root  $R_o(t)$ ,

169 The relationship between those three categories of the root population can  
170 be modelled as shown in Figure 1. Here we consider there is no death of  
171 young and mature roots. The computation of the root surface dynamics is

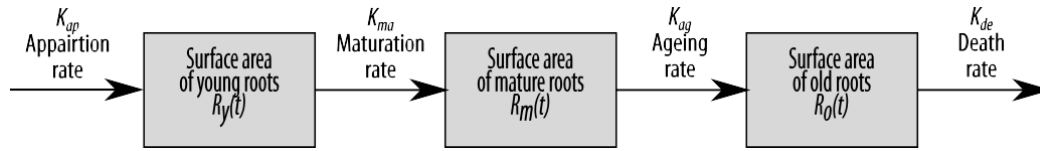


Figure 1: Conceptual model of the dynamic of root surface.  
 Possibility to consider only two categories for the root population.  $\kappa$  function of time?

172 given by the following equations, with  $R_y(t)$ ,  $R_m(t)$  and  $R_o(t)$ , the surface  
 173 areas occupied by young, mature, and old roots, respectively:

$$\frac{\partial R_y}{\partial t} = \kappa_{ap}(t) - \kappa_{ma}(t) \quad (6)$$

$$\frac{\partial R_m}{\partial t} = \kappa_{ma}(t) - \kappa_{ag}(t) \quad (7)$$

$$\frac{\partial R_o}{\partial t} = \kappa_{ag}(t) - \kappa_{de}(t), \quad (8)$$

174 with  $\kappa_{ap}(t)$  the apparition rate of young roots,  $\kappa_{ma}(t)$  the maturing rate of  
 175 young roots,  $\kappa_{ag}(t)$  the ageing rate of mature roots, and  $\kappa_{de}(t)$  the death rate  
 176 of old roots. No death of young and mature roots is considered. Thus the  
 177 changes in the total surface occupied by roots is:

$$\frac{\partial R}{\partial t} = \kappa_{ap}(t) - \kappa_{de}(t) \quad (9)$$

178 The general equation for the changes in porosity due to the population  
 179 dynamics of roots is function of  $\kappa_{ap}(t)$ ,  $\kappa_{ma}(t)$ ,  $\kappa_{ag}(t)$ , and  $\kappa_{de}(t)$ :

$$f(r) = -\kappa_{ap}(t) - \kappa_{ma}(t) + C_{ag}\kappa_{ag}(t) + \kappa_{de}(t). \quad (10)$$

180 This equation means that for each surface increase of young and mature  
 181 roots there is a direct proportional loss of porosity. Reversibly, for each  
 182 surface decrease of old roots by death, there is a direct proportional increase  
 183 of porosity. When mature roots are ageing and become old, the consequence  
 184 is the increase of porosity.  $dt_1$  is the time elapsed between the moment the  
 185 first root appears and the moment it starts narrowing.  $dt_2$  is the time elapsed  
 186 between  $dt_1$  and the lifetime of the plant or roots.  $dt_3$  is the time elapsed  
 187 between  $dt_2$  and the moment all dead roots disappeared or are degraded.  
 188 This time is soil moisture and biological activity dependent. As young and

189 mature roots have the same effect on soil porosity, we include the  
 190 and mature by extending the time. The previous equation then

$$f(r) = -K_{ma}(dt_1) + K_{ag}(dt_2) + R_{de}(dt_3) \tag{11}$$

191 From equations 10, 6, 7, 8, ??, we can deduce:

$$f(r) = kR_o(t) - \kappa_{ap}(t) - \frac{\partial R_m}{\partial t} \tag{12}$$

192  $R_v(t)$ ,  $R_m(t)$  and  $R_o(t)$  and their time derivatives can be obtained from  
 193 the experimental data at each time step. If no experimental data are available  
 194 general forms for  $\kappa_{ap}(t)$ ,  $\kappa_{ma}(t)$ , and  $\kappa_{ag}(t)$  must be proposed.

195 **2.4. Changes in porosity due to earthworms activity**

196 Jangorzo et al. (2013) showed that the intensity of earthworm activity  
 197 increase soil porosity. This activity is function of i) the number of earthworm,  
 198 ii) the quantity of organic matter and iii) the soil moisture. Many authors  
 199 have described the soil organic matter turnover and models we  
 200 Among these models we can announce the RothC (Coleman and  
 201 1999), StructureC Malamoud et al. (2009) and a module in  
 202 et al., 2015). The general equation of porosity evolution according to the  
 203 intensity of activity is as follows:

$$F(w) = k_{lw} \times I_w$$

204

$$I_w = f(I_w^{max} \times nb_w, \Theta, MO) \tag{14}$$

205 Where  $F(w)$  is the rate of porosity changes due to worm activity;  $I_w$  is the  
 206 total intensity of worm activity;  $I_w^{max}$  is the maximal intensity of worm  
 207 activity;  $k_{lw}$  is the conversion rate between the intensity of worm activity  
 208 and the proportion of pore surface;  $nb_w$  is the number of earthworms  
 209 the soil moisture or water potential and  $MO$  is the soil organic matter.

210 **2.4.1. Worm activity in relation with soil humidity**

211 In relation to earthworm development and activity, soil humidity is better  
 212 expressed as water potential due to the physiological characteristics of soil  
 213 organisms (Kretzschmar, 1991; Kretzschmar and Bruchou, 1991; Bruchou et al.,  
 214 2001; Moreau-Valancogne et al., 2013). Some studies showed

User  
2024-01-12 15:33:33

User  
2024-01-12 15:34:12

User  
2024-01-12 15:34:42

User  
2024-01-12 15:35:30

User  
2024-01-12 15:36:33

User  
2024-01-12 15:38:47

lw (index down)

215 of water potential on earthworm development (Kretzschmar and Bruchou,  
 216 1991; Holmstrup, 2001; Eriksen-Hamel and Whalen, 2006) and activity of  
 217 earthworm (Kretzschmar, 1991; Hindell et al., 1994; Daniel et al., 1996). All  
 218 those articles assess the development or the activity of *Aporrectodea spp.*,  
 219 which are endogeic or anecic earthworms. Other factors can be tested in  
 220 parallel (compaction, temperature). The earthworms activity is assessed via  
 221 their cast production. Kretzschmar (1991); Hindell et al. (1994); Daniel et al.  
 222 (1996) show the same pattern for the relationship between cast production  
 223 and water potential: no or a negligible cast production for water potentials  
 224 more negative than a base potential  $\Psi_b$  and then a linear increase of cast  
 225 production with increasing water potential until  $\Psi=0$ . The estimated values  
 226 of  $\Psi_b$  vary with species but indicate a narrow moisture tolerance range (Ta-  
 227 ble 2.4.1).  $\Psi_b$  seem to vary with the ecological type: around -20– -40 kPa  
 228 for anecic and around -10 kPa for endogeic.

Reference	Species	Ecological $\Psi_b$ type	(kPa)
Kretzschmar (1991)	<i>Aporrectodea longa</i>	anecic	-40
Hindell et al. (1994)	<i>Aporrectodea rosea</i>	endogeic	-10
id.	<i>Aporrectodea caliginosa</i>	endogeic	-10
id.	<i>Aporrectodea caliginosa f. trapezoides</i>	endogeic	-5
Daniel et al. (1996)	<i>Aporrectodea nocturna</i>	anecic	-20

Table 1: Value of the base water potential,  $\Psi_b$ , measured by different authors.

229 The relationship between the activity of *Lumbricus castaneus* (epi-anecic  
 230 worm, tested in Jangorzo (2013)) and the water potential shows the same  
 231 pattern as identified for anecic earthworms in the literature. So we hypothe-  
 232 sised that equations ?? and ?? can be inferred for *L. castaneus*. We assume  
 233 that the normalised earthworm activity is proportional to the normalised cast  
 234 production. Many equations were used to model the evolution of earthworms  
 235 activity as function of water potential but we are interested in that issuing  
 236 the cast production. For example Daniel et al. (1996) used an exponential  
 237 equation to predict the evolution of cast production by *Aporrectodea nocturna*.

$$C^*(P) = he^{(Pi)} \quad \text{for} \quad -0.06\text{MPa} \leq P \leq 0\text{MPa} \quad (15)$$

238 where  $C^*(P)$  is the transformed rate of cat production as a function of wa-  
 239 ter potential in MPa and  $h$  and  $i$  are constants. They assumed that cast

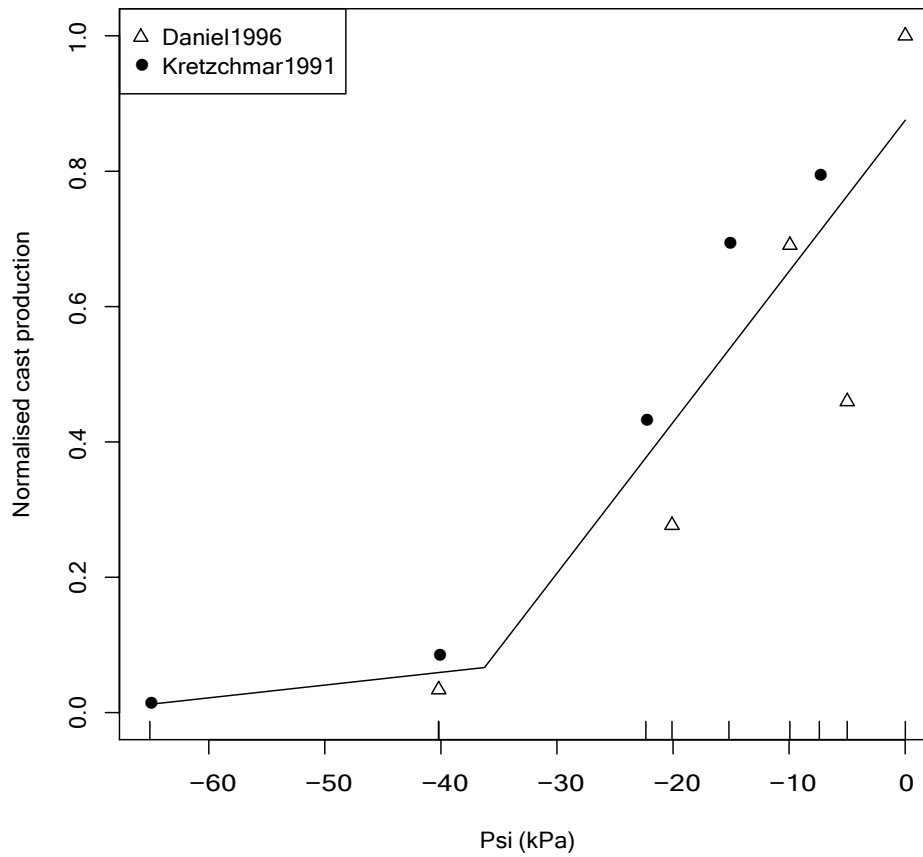


Figure 2: Model of the normalised cast production as a function of water potential for anecic earthworms. The data were extracted from Kretzschmar (1991) and Daniel et al. (1996). The fitted values are shown as points.

240 increased exponentially with the increase of water potential. Kaneda et al.  
 241 (2016) on the other hand used the modified Gompertz function expressed as  
 242 follows:

$$f(\Psi) = \zeta \exp^{-(\exp^{-(\Psi+\eta)/\vartheta})} \quad \text{for} \quad -90.6\text{kPa} < P < -2\text{kPa} \quad (16)$$

243 where  $f(P)$  stands for the soil aggregate formation rate-modifying factor for  
 244 soil moisture as a function of water potential  $\Psi$ , in kilopascal  $\zeta$ ,  $\eta$  and  $\vartheta$  are  
 245 constant experimental coefficients determining slope of the curve. They use  
 246 this function rather than Daniel's because their data showed a levelling-off  
 247 near the water potential 0 kPa. In contrary, experimental data obtained  
 248 by image analysis showed the increase of earthworm activity when water  
 249 potential increases (Jangorzo, 2013; Jangorzo et al., 2015). We therefore  
 250 used the Daniel's exponential equation to predict the evolution of earthworm  
 251 activity. This relation could be formalized by the normalized cast production  
 252 equation:

$$I_w(\Psi) = he^{(\Psi i)} \quad (17)$$

253 Here we consider the casts production as a result of the intense activity of  
 254 earthworm and this is proportional to the porosity production. However,  
 255 when earthworms burrow, they dig, ingest soil particles mixed with organic  
 256 matter that they excrete like casts. So, the cast produced are proportional to  
 257 the void created in the soil. Say  $k_w$  the coefficient indicating the conversion  
 258 between  $I_w$  and porosity. We assume that  $0 < k_w < 1$  as it is a ratio between  
 259 the  $I_w$  and the  $I_w^{max}$ . It means that not all the casts produced are equivalent  
 260 to the porosity created.

261 **2.4.2. Worm activity in relation with number of earthworms**

262 Most of experiments were undertaken with a single individual of earth-  
 263 worm. The effect of many individuals is not arithmetic but it has been shown  
 264 that more the number of earthworm is high, greater is the intensity and so  
 265 the porosity created (Jangorzo et al., 2015). However, 17 could be rearranged  
 266 as follows:

$$I_w(\Psi) = nb_w \times he^{(\Psi i)}$$

267 Where  $nb_w$  is the number of earthworms

User  
 2024-01-13 09:40:36  
 -----  
 space (18)

User  
 2024-01-13 09:40:57  
 -----

268 **2.4.3. Worm activity in relation with organic matter content**

269 Organic matter is used by earthworms for feeding and they burrow in  
 270 order to find food. In this model, we assume that the organic matter content  
 271 is constant as the quantity introduced in the system does not vary. However,  
 272 the variation of earthworm activity as function of organic matter is equal to  
 273 zero as well as that of soil temperature.

274 Combining the equations 13,14 and 18 we can write the general  
 275 of porosity evolution as function of earthworms activity as follows

$$F(w) = k_l \times n_b \times h_e^{(\psi_i)} \tag{19}$$

276 **2.5. Porosity disappearance**

277 We suggest that a proportion of the total porosity disappeared at each  
 278 time step: Two processes induce porosity disappearance according to our  
 279 assumption: i) water loading charge during wetting or watering and soil  
 280 fauna (earthworms) when burrowing.

$$D_P = f(\Theta, I_w) \tag{20}$$

281 **2.5.1. Porosity disappearance due to watering**

282 When water is added in a structured soil, according to the stability of  
 283 the soil, this water induce extinction of some aggregates. During water flow,  
 284 these particles are transport deep in the soil through porosity. At the limit of  
 285 water infiltration, these particles are deposited creating fillings. This process  
 286 lead to the decrease of porosity. However a successive watering without  
 287 bioturbation lead undoubtedly to a disappearance of soil macropores. Say  
 288  $P_0$  the porosity of the system at  $T_0$ . After the first watering, the porosity  
 289 decrease into  $P_1$  at  $T_1$ . After  $n$  series of watering we have a porosity of  $P_n$ .  
 290 The total porosity that disappears is:

$$\Delta(P_\Theta) = \sum_1^n (P_{n+1} - P_n) \tag{21}$$

291 Where  $P$  is the porosity,  $n$  the number of watering series and the  $\Theta$  means  
 292 that the decrease is due to watering.

293 **2.5.2. Porosity disappearance due to earthworms activity**

294 In presence of earthworms, we assume that the decrease of porosity due  
 295 to watering is null as during burrowing earthworm are willing to extract the

296 filings. The only action that decreases porosity is the deposit of casts in  
 297 burrows. This action depends on how many times an earthworms passes in  
 298 a burrow. Say  $P_0$  the porosity of the system at  $T_0$ . After the first passage  
 299 (burrowing), the porosity decreases into  $P_1$  at  $T_1$ . After  $n$  series of burrowing  
 300 we have a porosity of  $P_n$ . The total porosity that disappears is:

$$\Delta(P_w) = \sum_1^n (P_{n+1} - P_n) \tag{22}$$

301 Where  $P$  is the porosity,  $n$  the number of earthworm activity (burrowing)  
 302 and the  $w$  means that the decrease is due to burrowing.

303 The solutions of equations 21 and 22 could be obtained using the least mean  
 304 square methods as experienced by Daniel (1991); Daniel et al. (1996). The  
 305 principle of least mean square method is formalized by (Stocker et al., 2002)  
 306 which stipulates that: Given a function  $y(x) = y(x; a)$  dependant on a pa-  
 307 rameter  $a$  and  $n$  couples of values  $(x_i; y_i)$ , the optimal parameter  $a$  is defined  
 308 by the Gauss function as follows:

$$\sum_i (y_i - y(x_i; a))^2 = Min_a \tag{23}$$

309 The idea behind this function is that it minimise the variable  $a$  and tends to a  
 310 residual. In the case of our study, it means that the disappearance of porosity  
 311 due to watering and earthworm activity is minimised. However the porosity  
 312 decreases at each time step and at each watering, but due to the action of  
 313 plants roots or burrowing, the decrease is compensate latter particularly by  
 314 earthworms. This is why, unless this temporary decrease, the surface area of  
 315 porosity increases with time. This can be formalised as follows:

316 **2.6. Submodels integration**

317 In our approach, we assumed that different factors acted successively in  
 318 soil structuring. Beginning by the soil moisture which is the limiting factor  
 319 to biological activity. Second plants find ideal conditions to develop and then  
 320 soil fauna like earthworms. To maintain an equilibrium, a proportion of soil  
 321 structure disappears due to the same structuring agents, primarily water.

User  
 2024-01-13 09:42:15

---

Successively in  
 limiting factor  
 develop and then  
 proportion of soil  
 primarily water.

322 Rearranging 1 we obtained:

$$\frac{dP}{dt} = [(I_w^{max} \times nb_w)^{-zv} \times \begin{cases} 0,0224\psi + 0,8764, & \text{for } \psi < \Psi_b \\ 0,0019\psi + 0,1379, & \text{for } \psi > \Psi_b \end{cases} \quad (24)$$

$$+ [(3 + \eta_{ar}) - \frac{(D_b \gamma r + D_b a r + D_b o r)}{D_s}] \quad (25)$$

$$+ [ \int_1^n \frac{D_s}{\epsilon + 1} (\epsilon + \Theta^{-q}) ] - D_p \quad (26)$$

### 323 3. Model implementation

324 An experiment was set up in a climate chamber where the effect of  
 325 wetting-drying cycle, plant roots and earthworm activity on soil structure  
 326 has been studied. This experiment was run during 14 months; images were  
 327 recorded using Soilinsight (INRA, 2015), a dispositive of *insitu* monitoring  
 328 of soil structure developed by Jangorzo (2013) and soil structure parameters  
 329 were quantified by image analysis (Jangorzo et al., 2013, 2014, 2015). Three  
 330 replicates of each factor were realized. The experimental design was fully de-  
 331 scribed in Jangorzo (2013).

#### 332 3.1. Initial conditions

333 At the beginning of the experiment  $t = 0$ , the surface areas of porosity  
 334 and aggregates were quantified but the surface area of roots was null as well  
 335 as the earthworm activity.

$$P(t = 0) = P_0 \quad (27)$$

$$r(t = 0) = 0 \quad (28)$$

$$I_w(t = 0) = 0 \quad (29)$$

#### 336 3.2. Swelling-Shrinkage parameters

337 The mesocosm used in this experiment were filled with a constructed  
 338 Technosol 500  $\mu\text{m}$  sieved. The soil was made by a mixture of Treated Indus-  
 339 trial Soil (TIS) and Paper mill-Sludge (PS). At the top of the cosm a thin  
 340 layer of compost was layed out. Cosms were first moistened by capillarity  
 341 uptake until saturation and gravimetric water content at field capacity was  
 342 measured by weighing. Then four wetting-drying cycles where applied. After  
 343 saturation, the system was let for drying until 20%. Then it is wetted un-  
 344 til saturation and the excess water was collected as leachate. Regularly the

345 cosms were weighed to determine the water content. Based on these infor-  
 346 mation the relation between matric potential and gravimetric water content  
 347 was establish using hydrus. Images were analysed and cracks parameters  
 348 were quantified.

### 349 3.3. Plant roots parameters

350 In other cosms, four seeds of *Lupinus albus* were sown and root devel-  
 351 opment is monitored as described by Jangorzo et al. (2015). Fours days  
 352 after the beginning of the experiment, the first roots appeared. Say  $D_1$  this  
 353 date. Roots continue growing during time and the surface is calculated by  
 354 image analysis. By comparing different images generated, we identify the  
 355 time when roots stop growing. Say  $D_2$  this day. Then the  $dt_1$  is deduced as  
 356 follows :  $dt_1 = D_2 - D_1$ . The variation of roots surface according to time  
 357  $\frac{\partial R_m}{\partial t}$  is calculated. The experiment continued running and at a moment plant  
 358 roots were dead unless the system was watered. Say  $D_3$  this date. The time  
 359 elapsed during roots narrowing  $dt_2 = D_3 - D_2$  is determined. Knowing  $\frac{\partial R_o}{\partial t}$   
 360 the total surface of dead roots is quantified, then the variation rate  $\frac{\partial R_o}{\partial t}$  is  
 361 calculated. The rate of dead roots degradation is determined as soon as roots  
 362 disappeared. This coefficient can also be determined using the equation of  
 363 Lafolie used in Vsoil.

### 364 3.4. Earthworms activity parameters

365 In cosms containing plant roots, were introduced six individuals ( $nb_w$ ) of  
 366 *Lumbricus castaneus*. The soil moisture was maintained in a range between  
 367 60% field capacity and 80% filed capacity. Using hydrus, this moisture con-  
 368 tent is equivalent to a corresponding suction  $\Psi$ . As in the previous systems,  
 369 images were generated each two hours what allows us to monitor the earth-  
 370 worm activity. The different operations recorded are the number of visible  
 371 actions made by a worm: i) creating a burrow, ii) filing a burrow, iii) en-  
 372 larging burrow; iv) unchanged burrow (Jangorzo et al., 2015). Then the  
 373 intensity of earthworms activity  $I_w$  was determined knowing the number of  
 374 individuals and the time elapsed. Moreover, image were analysed to quantify  
 375 the evolution of soil porosity.

## 376 4. Conclusion and perspectives

377 Based on an innovative experimental set-up of soil observation and quan-  
 378 tification, we proposed a conceptual model of soil porosity dynamics under

379 the influence of three aggregation factors. For this, three agents were exper-  
 380 imented: wetting-drying cycle for environmental factor, *Lupinus albus* for  
 381 plant roots and *Lumbricus castaneus* for soil fauna. To validate this model,  
 382 it is important to set up a new experiment and resolve the different equations  
 383 by computing them.

384 **Appendix A. Variable definitions**

385 All the variables used in the model are summarised in Table A.2.

Var.	Definition	Units	Source
$a_{r_y}$	Apparition rate of young roots	$\text{mm}^2 \times 10^{-2}$ $\text{mm}^{-2} \times \text{h}^{-1}$	
$A(t)$	Surface area of the soil aggregates in proportion to the total surface of the picture	$\text{mm}^2 \times 10^{-2}$ $\text{mm}^{-2}$	Obtained by image analysis on experimental data (Jangorzo, 2013)
$d_{r_d}$	Degradation rate of dead roots	$\text{mm}^2 \times 10^{-2}$ $\text{mm}^{-2} \times \text{h}^{-1}$	
$D_p$	Destruction rate of the porosity	$\text{mm}^2 \times 10^{-2}$ $\text{mm}^{-2} \times \text{h}^{-1}$	Literature review on soil compaction and collapse, experimental framework
$\vartheta$	Rate of porosity changes due to soil humidity (wetting and drying cycles)	$\text{mm}^2 \times 10^{-2}$ $\text{mm}^{-2} \times \text{h}^{-1}$	
$f(w)$	Rate of porosity changes due to worm activity	$\text{mm}^2 \times 10^{-2}$ $\text{mm}^{-2} \times \text{h}^{-1}$	
$f(r)$	Rate of porosity changes due to root dynamics	$\text{mm}^2 \times 10^{-2}$ $\text{mm}^{-2} \times \text{h}^{-1}$	
$I_w$	Total intensity of worm activity	Number of worm actions per hour	Computed by image analysis from experimental data

**Table A.2 – continued from previous page**

<b>Var.</b>	<b>Definition</b>	<b>Units</b>	<b>Source</b>
$I_w^{\max}$	Maximal intensity of worm activity	Number of worm actions per hour and per individual	Computed by image analysis from experimental data Jangorzo (2013)
$k$	Factor of porosity destruction (collapse due to humidity)	Dimensionless	Calibration or literature review
$k_{I_w}$	Conversion rate between the intensity of worm activity and pore surface proportion	$\text{mm}^2 \times 10^{-2}$ $\text{mm}^{-2}$ per worm action	
$k_{r_d}$	Conversion rate between the surface of degraded roots and the pore surface	Dimensionless	Calibration or computation from experimental data Jangorzo (2013)
$k_{r_y}$	Conversion rate between the surface area of new young roots and the pore surface area (proportion of porosity occupied by the surface area of new young roots)	Dimensionless	Calibration or computation from experimental data Jangorzo (2013)
$k_{r_y \rightarrow o}$	Conversion rate between the surface area of new old roots and the pore surface area	Dimensionless	Calibration or computation from experimental data Jangorzo (2013)
$k_{r_o \rightarrow d}$	Conversion rate between the surface area of new dead roots and the pore surface area	Dimensionless	Calibration or computation from experimental data Jangorzo (2013)

**Table A.2 – continued from previous page**

<b>Var.</b>	<b>Definition</b>	<b>Units</b>	<b>Source</b>
$k_{\theta}$	Conversion rate between humidity variations and pore surface proportion	$\text{mm}^2 \times 10^{-2}$ $\text{mm}^{-2}$ per soil humidity unit	Literature review on shrinking, experimental framework
$m_{r_d}$	Death rate/mortality of old roots	$\text{mm}^2 \times 10^{-2}$ $\text{mm}^{-2} \times \text{h}^{-1}$	
MO	Soil organic matter content	$\text{g} \cdot \text{g}^{-1}$	Literature review
$nb_w$	Number of earthworms	Individuals	
$P(t)$	Surface area of the porosity ( $> 50 \mu\text{m}$ ) in proportion to the total surface of the picture	$\text{mm}^2 \times 10^{-2}$ $\text{mm}^{-2}$	Obtained by image analysis on experimental data (Jangorzo, 2013)
$P_0$	Surface area of the porosity ( $> 50 \mu\text{m}$ ) in proportion to the total surface of the picture at the initial time $t = 0$	$\text{mm}^2 \times 10^{-2}$ $\text{mm}^{-2}$	Obtained by image analysis on experimental data (Jangorzo, 2013)
$R(t)$	Total surface area occupied by roots in proportion to the total surface of the picture	$\text{mm}^2 \times 10^{-2}$ $\text{mm}^{-2}$	Obtained by image analysis on experimental data (Jangorzo, 2013)
$R_o(t)$	Surface area with old roots in proportion to the total surface of the picture	$\text{mm}^2 \times 10^{-2}$ $\text{mm}^{-2}$	Obtained by image analysis on experimental data (Jangorzo, 2013)
$R_m(t)$	Surface area with mature roots in proportion to the total surface of the picture	$\text{mm}^2 \times 10^{-2}$ $\text{mm}^{-2}$	Obtained by image analysis on experimental data (Jangorzo, 2013)

**Table A.2 – continued from previous page**

<b>Var.</b>	<b>Definition</b>	<b>Units</b>	<b>Source</b>
$R_y(t)$	Surface area with young roots in proportion to the total surface of the picture	$\text{mm}^2 \times 10^{-2}$ $\text{mm}^{-2}$	Obtained by image analysis on experimental data (Jangorzo, 2013)
$t$	Time	Hour (h)	Experimental time step is 2 h for a total length of the experiment of 14 months
$v_{ry}$	Ageing rate of young roots (conversion in old roots)	$\text{mm}^2 \times 10^{-2}$ $\text{mm}^{-2} \times \text{h}^{-1}$	
$K_{d_r}$	Coefficient of root degradation (proportion of root degradation in relation to the population of dead roots)	$\text{h}^{-1}$	Calibration or literature review
$\Theta$	Soil humidity or matric potential ( $\Psi$ )	Units in relation with the chosen variables	Literature review

Table A.2: Description of the used variables.

Var. : Variables.

387 **References**

388 Braudeau, E., Mohtar, R. H., Mar. 2006. Modeling the Swelling Curve for  
 389 Packed Soil Aggregates Using the Pedostructure Concept. Soil Science  
 390 Society of America Journal 70 (2), 494–502.

391 URL [https://dl.sciencesocieties.org/publications/sssaj/  
 392 abstracts/70/2/494](https://dl.sciencesocieties.org/publications/sssaj/abstracts/70/2/494)

393 Chertkov, V. Y., 2012a. An integrated approach to soil structure, shrinkage,  
 394 and cracking in samples and layers. Geoderma 173–174 (0), 258–273.

- 395 URL [http://www.sciencedirect.com/science/article/pii/](http://www.sciencedirect.com/science/article/pii/S0016706112000341)  
396 S0016706112000341
- 397 Chertkov, V. Y., Aug. 2012b. Physical modeling of the soil swelling curve  
398 vs. the shrinkage curve. *Advances in Water Resources* 44 (Supplement C),  
399 66–84.  
400 URL [http://www.sciencedirect.com/science/article/pii/](http://www.sciencedirect.com/science/article/pii/S0309170812001078)  
401 S0309170812001078
- 402 Chertov, O., Shaw, C., Shashkov, M., Komarov, A., Bykhovets, S., Shanin,  
403 V., Grabarnik, P., Frolov, P., Kalinina, O., Pripulina, I., Zubkova, E., Feb.  
404 2017. Romul\_hum model of soil organic matter formation coupled with  
405 soil biota activity. III. Parameterisation of earthworm activity. *Ecological*  
406 *Modelling* 345 (Supplement C), 140–149.  
407 URL [http://www.sciencedirect.com/science/article/pii/](http://www.sciencedirect.com/science/article/pii/S0304380016302368)  
408 S0304380016302368
- 409 Coleman, K., Jinkinson, S, D., 1999. RothC-26.3. A Model for the Turnover  
410 of Carbon in Soil: Model Description and User's Guide. Lawes Agricultural  
411 Trust.
- 412 Coppola, A., Comegna, A., Dragonetti, G., Gerke, H. H., Basile, A.,  
413 Sep. 2015. Simulated Preferential Water Flow and Solute Transport in  
414 Shrinking Soils. *Vadose Zone Journal* 14 (9).  
415 URL [https://dl.sciencesocieties.org/publications/vzj/](https://dl.sciencesocieties.org/publications/vzj/abstracts/14/9/vzj2015.02.0021)  
416 [abstracts/14/9/vzj2015.02.0021](https://dl.sciencesocieties.org/publications/vzj/abstracts/14/9/vzj2015.02.0021)
- 417 Coppola, A., Gerke, H. H., Comegna, A., Basile, A., Comegna, V., Aug.  
418 2012. Dual-permeability model for flow in shrinking soil with dominant  
419 horizontal deformation. *Water Resources Research* 48 (8), W08527.  
420 URL [http://onlinelibrary.wiley.com/doi/10.1029/2011WR011376/](http://onlinelibrary.wiley.com/doi/10.1029/2011WR011376/abstract)  
421 [abstract](http://onlinelibrary.wiley.com/doi/10.1029/2011WR011376/abstract)
- 422 Croney, D., Coleman, J. D., Jan. 1954. Soil structure in relation to soil  
423 suction (pF). *Journal of Soil Science* 5 (1), 75–84.  
424 URL [http://onlinelibrary.wiley.com/doi/10.1111/j.1365-2389.](http://onlinelibrary.wiley.com/doi/10.1111/j.1365-2389.1954.tb02177.x/abstract)  
425 [1954.tb02177.x/abstract](http://onlinelibrary.wiley.com/doi/10.1111/j.1365-2389.1954.tb02177.x/abstract)
- 426 Daniel, O., Dec. 1991. Leaf-litter consumption and assimilation by juveniles  
427 of *Lumbricus terrestris* L. (*Oligochaeta*, *Lumbricidae*) under different en-

- 428 vironmental conditions. *Biology and Fertility of Soils* 12 (3), 202–208.  
429 URL <https://link.springer.com/article/10.1007/BF00337203>
- 430 Daniel, O., Kohli, L., Schuler, B., Zeyer, J., APR 1996. Surface cast produc-  
431 tion by the earthworm *Aporrectodea nocturna* in a pre-alpine meadow in  
432 Switzerland. *Biology and Fertility of Soils* 22 (1–2), 171–178.
- 433 Eriksen-Hamel, N. S., Whalen, J. K., Jul. 2006. Growth rates of *Apor-*  
434 *rectodea caliginosa* (Oligochaeta: Lumbricidae) as influenced by soil  
435 temperature and moisture in disturbed and undisturbed soil columns.  
436 *Pedobiologia* 50 (3), 207–215.  
437 URL [http://www.sciencedirect.com/science/article/pii/](http://www.sciencedirect.com/science/article/pii/S0031405605001356)  
438 [S0031405605001356](http://www.sciencedirect.com/science/article/pii/S0031405605001356)
- 439 Greco, R., Dec. 2002. Preferential flow in macroporous swelling soil with  
440 internal catchment: model development and applications. *Journal of*  
441 *Hydrology* 269 (3), 150–168.  
442 URL [http://www.sciencedirect.com/science/article/pii/](http://www.sciencedirect.com/science/article/pii/S0022169402002159)  
443 [S0022169402002159](http://www.sciencedirect.com/science/article/pii/S0022169402002159)
- 444 Hindell, R., McKenzie, B., Silvapulle, M., Tisdall, J., 1994. Relationships  
445 between casts of geophagous earthworms (*Lumbricidae*, *Oligochaeta*) and  
446 matric potential. *Biol. Fertil. Soils* 18 (2), 119–126.
- 447 Holmstrup, M., Jul. 2001. Sensitivity of life history parameters in the earth-  
448 worm *Aporrectodea caliginosa* to small changes in soil water potential.  
449 *Soil Biology and Biochemistry* 33 (9), 1217–1223.  
450 URL [http://www.sciencedirect.com/science/article/pii/](http://www.sciencedirect.com/science/article/pii/S0038071701000268)  
451 [S0038071701000268](http://www.sciencedirect.com/science/article/pii/S0038071701000268)
- 452 Huot, H., Simonnot, M. O., Watteau, F., Marion, P., Yvon, J., De Donato,  
453 P., Morel, J. L., 2014. Early transformation and transfer processes in a  
454 Technosol developing on iron industry deposits. *Eur. J. Soil Sci.* 65 (4),  
455 470–484.  
456 URL <http://dx.doi.org/10.1111/ejss.12106>
- 457 INRA, May 2015. Soilinsight® : Un voyage au cœur des sols.  
458 URL [http://www.nancy.inra.fr/Toutes-les-actualites/](http://www.nancy.inra.fr/Toutes-les-actualites/Soilinsight-R)  
459 [Soilinsight-R](http://www.nancy.inra.fr/Toutes-les-actualites/Soilinsight-R)

- 460 Jangorzo, N. S., Schwartz, C., Watteau, F., 2014. Image analysis of soil thin  
461 sections for a non-destructive quantification of aggregation in the early  
462 stages of pedogenesis. *European Journal of Soil Science* 65 (4), 485–498.  
463 URL <http://dx.doi.org/10.1111/ejss.12110>
- 464 Jangorzo, N. S., Watteau, F., Hajos, D., Schwartz, C., 2015. Nondestructive  
465 monitoring of the effect of biological activity on the pedogenesis of a Techno-  
466 sol. *Journal of Soils and Sediments* 15 (8), 1705–1715.  
467 URL <https://doi.org/10.1007/s11368-014-1008-z>
- 468 Jangorzo, N. S., Watteau, F., Schwartz, C., 2013. Evolution of the pore  
469 structure of constructed Technosols during early pedogenesis quantified  
470 by image analysis. *Geoderma* 207-208 (0), 180–192.  
471 URL [http://www.sciencedirect.com/science/article/pii/  
472 S0016706113001705](http://www.sciencedirect.com/science/article/pii/S0016706113001705)
- 473 Jangorzo, S. N., Feb. 2013. Quantification du processus d'agrégation dans les  
474 Technosols. Ph.D. thesis, Université de Lorraine, Nancy.  
475 URL <http://www.theses.fr/2013LORR0004>
- 476 Jones, C. G., Lawton, J. H., Shachak, M., 1994. Organisms as Ecosystem  
477 Engineers. In: *Ecosystem Management*. Springer, New York, NY, pp.  
478 130–147, doi: 10.1007/978-1-4612-4018-1\_14.  
479 URL [https://link.springer.com/chapter/10.1007/  
480 978-1-4612-4018-1\\_14](https://link.springer.com/chapter/10.1007/978-1-4612-4018-1_14)
- 481 Kaneda, S., Ohkubo, S., Wagai, R., Yagasaki, Y., Aug. 2016. Soil temper-  
482 ature and moisture-based estimation of rates of soil aggregate formation  
483 by the endogeic earthworm *Eisenia japonica* (Michaelsen, 1892). *Biology  
484 and Fertility of Soils* 52 (6), 789–797.  
485 URL [https://link.springer.com/article/10.1007/  
486 s00374-016-1119-3](https://link.springer.com/article/10.1007/s00374-016-1119-3)
- 487 Komarov, A., Chertov, O., Bykhovets, S., Shaw, C., Nadporozhskaya,  
488 M., Frolov, P., Shashkov, M., Shanin, V., Grabarnik, P., Priputina,  
489 I., Zubkova, E., Feb. 2017. Romul hum model of soil organic matter  
490 formation coupled with soil biota activity. I. Problem formulation, model  
491 description, and testing. *Ecological Modelling* 345 (Supplement C),  
492 113–124.

- 493 URL [http://www.sciencedirect.com/science/article/pii/](http://www.sciencedirect.com/science/article/pii/S0304380016303088)  
494 [S0304380016303088](http://www.sciencedirect.com/science/article/pii/S0304380016303088)
- 495 Konrad, J. M., Ayad, R., 1997. A idealized framework for the analysis of co-  
496 hesive soils undergoing desiccation. *Canadian Geotechnical Journal* 34 (4),  
497 477–488.  
498 URL <https://doi.org/10.1139/t97-015>
- 499 Kretzschmar, A., Apr. 1991. Burrowing ability of the earthworm *Aporrec-*  
500 *todea longa* limited by soil compaction and water potential. *Biology and*  
501 *Fertility of Soils* 11 (1), 48–51.  
502 URL <https://link.springer.com/article/10.1007/BF00335834>
- 503 Kretzschmar, A., Bruchou, C., Dec. 1991. Weight response to the soil water  
504 potential of the earthworm *Aporrectodea longa*. *Biology and Fertility of*  
505 *Soils* 12 (3), 209–212.  
506 URL <https://link.springer.com/article/10.1007/BF00337204>
- 507 Lafolie, F., Cousin, I., Mollier, A., Pot, V., Maron, P., Noguier, C., Moitrier,  
508 N., Beudez, N., 2015. Which benefits in the use of a modeling platform:  
509 The VSoil example. In: *Geophys. Res. Vienna*, p. 1.
- 510 Malamoud, K., McBratney, A. B., Minasny, B., Fiel, D. J., 2009. Modelling  
511 how carbon affects soil structure. *Geoderma*, 19–26.
- 512 Moreau-Valancogne, P., Bertrand, M., Holmstrup, M., Roger-Estrade, J.,  
513 AUG 2013. Integration of thermal time and hydrottime models to describe  
514 the development and growth of temperate earthworms. *Soil Biology &*  
515 *Biochemistry* 63, 50–60.
- 516 Peng, X., Horn, R., Feb. 2007. Anisotropic shrinkage and swelling of some  
517 organic and inorganic soils. *European Journal of Soil Science* 58 (1),  
518 98–107.  
519 URL [http://onlinelibrary.wiley.com/doi/10.1111/j.1365-2389.](http://onlinelibrary.wiley.com/doi/10.1111/j.1365-2389.2006.00808.x/abstract)  
520 [2006.00808.x/abstract](http://onlinelibrary.wiley.com/doi/10.1111/j.1365-2389.2006.00808.x/abstract)
- 521 Six, J., Bossuyt, H., Degryze, S., Denef, K., 2004. A history of research on  
522 the link between (micro) aggregates, soil biota, and soil organic matter  
523 dynamics. *Soil & Tillage Research* 1 (79), 7–31.

- 524 Smiles, D. E., 2000. Hydrology of swelling soils: a review. *Soil Research*  
525 38 (3), 501–521.  
526 URL <http://www.publish.csiro.au/sr/SR99098>
- 527 Stewart, R., E Rupp, D., Abou Najm, M., Selker, J., Mar. 2016. A Unified  
528 Model for Soil Shrinkage, Subsidence, and Cracking. *Vadose Zone Journal*  
529 15, 1–15.
- 530 Stocker, H., Bossler, V., Marcello, S., 2002. *Toutes les mathématiques et les*  
531 *bases de l’informatique*, 2002nd Edition. Dunod, Paris.  
532 URL [https://www.dunod.com/sciences-techniques/](https://www.dunod.com/sciences-techniques/toutes-mathematiques-et-bases-informatique)  
533 [toutes-mathematiques-et-bases-informatique](https://www.dunod.com/sciences-techniques/toutes-mathematiques-et-bases-informatique)
- 534 Tessier, D., 1984. Etude expérimentale de l’organisation des matériaux  
535 argileux : hydratation, gonflement et structuration au cours de la dess-  
536 iccation et de la réhumectation = Experimental study of organization of  
537 argillous materials: hydratation, swelling and structuration during desic-  
538 cation and humectation. Text, Université Paris VII, Paris.  
539 URL <http://cat.inist.fr/?aModele=afficheN&cpsidt=8481673>
- 540 Vereecken, H., Schnepf, A., Hopmans, J., Javaux, M., Or, D., Roose, T.,  
541 Vanderborght, J., Young, M., Amelung, W., Aitkenhead, M., Allison, S.,  
542 Assouline, S., Baveye, P., Berli, M., Brüggemann, N., Finke, P., Flury,  
543 M., Gaiser, T., Govers, G., Ghezzehei, T., Hallett, P., Hendricks Franssen,  
544 H., Heppell, J., Horn, R., Huisman, J., Jacques, D., Jonard, F., Kollet,  
545 S., Lafolie, F., Lamorski, K., Leitner, D., McBratney, A., Minasny, B.,  
546 Montzka, C., Nowak, W., Pachepsky, Y., Padarian, J., Romano, N., Roth,  
547 K., Rothfuss, Y., Rowe, E., Schwen, A., Šimůnek, J., Tiktak, A., Van Dam,  
548 J., van der Zee, S., Vogel, H., Vrugt, J., Wöhling, T., Young, I., 2016.  
549 Modeling Soil Processes: Review, Key Challenges, and New Perspectives.  
550 *Vadose Zone Journal* 15 (5).  
551 URL <http://dx.doi.org/10.2136/vzj2015.09.0131>
- 552 Wang, G., Wei, X., Oct. 2014. Modeling swelling–shrinkage behavior  
553 of compacted expansive soils during wetting–drying cycles. *Canadian*  
554 *Geotechnical Journal* 52 (6), 783–794.  
555 URL [http://www.nrcresearchpress.com/doi/abs/10.1139/](http://www.nrcresearchpress.com/doi/abs/10.1139/cgj-2014-0059)  
556 [cgj-2014-0059](http://www.nrcresearchpress.com/doi/abs/10.1139/cgj-2014-0059)

557 Zangerlé, A., Pando, A., Lavelle, P., 2011. Do earthworms and roots coop-  
558 erate to build soil macroaggregates? A microcosm experiment. *Geoderma*  
559 167-168 (0), 303–309.  
560 URL [http://www.sciencedirect.com/science/article/pii/](http://www.sciencedirect.com/science/article/pii/S0016706111002709)  
561 [S0016706111002709](http://www.sciencedirect.com/science/article/pii/S0016706111002709)